ASSESSING THE IMPACT OF FORESTS ON LOCAL WIND CONDITIONS IN ARCHIPELAGOS: A CFD STUDY

Ashvinkumar Chaudhari* and Eero Immonen
Computational Engineering and Analysis (COMEA)
Turku University of Applied Sciences
20520 Turku, Finland
* Email: Ashvin.Chaudhari@turkuamk.fi

Mikael Manngård, Johan Westö and Dennis Bengs
Research, Development, and Innovation,
Novia University of Applied Sciences
20100 Turku, Finland

KEYWORDS

CFD, Archipelagos, Complex terrains, Forest effects, Wind flow analysis, Turbulence.

ABSTRACT

Ship fairways in archipelagos pass close to small islands with complex terrain and forests. In such areas, local wind conditions deviate from regional forecasts, creating a complex and challenging environment when navigating large vessels. In this article, we carried out Computational Fluid Dynamics (CFD) simulations for wind flows over a site in the Turku Archipelago, in Finland. We assessed local wind conditions along the fairway with the intent of improving safe passage for large vessels. All simulations were carried out with and without the surrounding forests to elucidate the role of forests in shaping the local wind and turbulence conditions over the site. Our results show that in some regions of the fairway, forests can lower the wind speed to one-third of the magnitude obtained by using terrain-only models. Moreover, turbulence can locally be increased sixfold. We expect that these results will facilitate the development of new smart fairways for ensuring safe navigation through the archipelago in the future.

INTRODUCTION

Archipelagos in the Northern Baltic Sea constitute complex environments for navigation with specific challenges for safe passage. The fairway passes close to islands and forested areas, with currents and winds being strongly influenced by the surrounding terrains. Local wind conditions, for example, might deviate strongly from the regional forecasts, making it difficult to predict external forces on a vessel beforehand. Safe navigation thus requires access to the tacit knowledge of experienced sea pilots and captains familiar with the area. Navigational safety is consequently dependent on knowledge in the form of human experience acquired over the years or even a lifetime. We envision that smart fairway will complement human experience in the future, and that navigational safety and situational awareness will be improved through data-driven and simulation-informed decision-making techniques. The future smart fairways could be seen as digital twins (Kritzinger et al., 2018; Jones et al., 2020) of the environment that enriches the tacit knowledge acquired by humans through simulations. For example, knowledge of local wind conditions would make it possible to simulate forces and torques on vessels (Koop et al., 2012; Janssen et al., 2017), and to evaluate the operational limits of vessels in varying wind conditions as they traverse the fairway.

A key step towards realizing the above vision is to acquire knowledge about local wind conditions along the fairway. Weather forecasts and weather stations together provide an estimate of the regional wind conditions, but this information needs to be refined to local conditions along the fairway. Computational Fluid Dynamics (CFD) simulations constitute a promising approach for accomplishing this goal, as such simulations have previously been successfully used to predict localized wind flows over complex terrains (Chaudhari et al., 2014; Blocken et al., 2015; Conan et al., 2016; Chaudhari et al., 2016; Dhunny et al., 2017; Temel et al., 2018; Chaudhari et al., 2018; Ravensbergen et al., 2020). However, earlier studies were mainly carried out for wind resources assessment over terrains without forests, or in port areas dominated by man-made structures (Ricci et al., 2019, 2020, 2023). In archipelagos, wind flows are instead expected to be influenced by the combined effects of surrounding terrain and forests. As forests are porous, a certain amount of wind penetrates through them. As a result, the wind conditions, after a forest patch, would be different as compared to the flow behind a solid terrain. There is thus a need for CFD studies estimating and charting local wind conditions along the fairway in an archipelago. Especially so, as currents also often depend on the wind conditions (Kanarik et al., 2018). Immonen et al. (2022) recently took an initial step by developing a framework to create automatic mesh generation for flow simulations over complex terrains in an archipelago. However, this framework still only included the terrain effects and additional work is required to include the presence of forests.

The main contributions of this work are in, 1) implementing an open-source simulation framework that incorporates both terrain and forest effects in wind-flow simulations, and 2) assessing the impact of forests on the local wind flows in archipelagos with complex terrain. We performed wind-flow simulations for a portion of the fairway in the Finnish archipelago. The studied site is shown in Figure 1 and is located just outside of the Port of Turku.

CFD MODELING

Numerical Models

The steady-state Reynold's Averaged Navier-Stokes (RANS) equations, together with the Realizable $\kappa - \epsilon$

Communications of the ECMS, Volume 37, Issue 1,
Proceedings, ©ECMS Enrico Vicario, Romeo Bandinelli,
Virginia Fani, Michele Mastroianni (Editors) 2023
ISBN: 978-3-937436-80-7/978-3-937436-79-1 (CD) ISSN 2522-2414

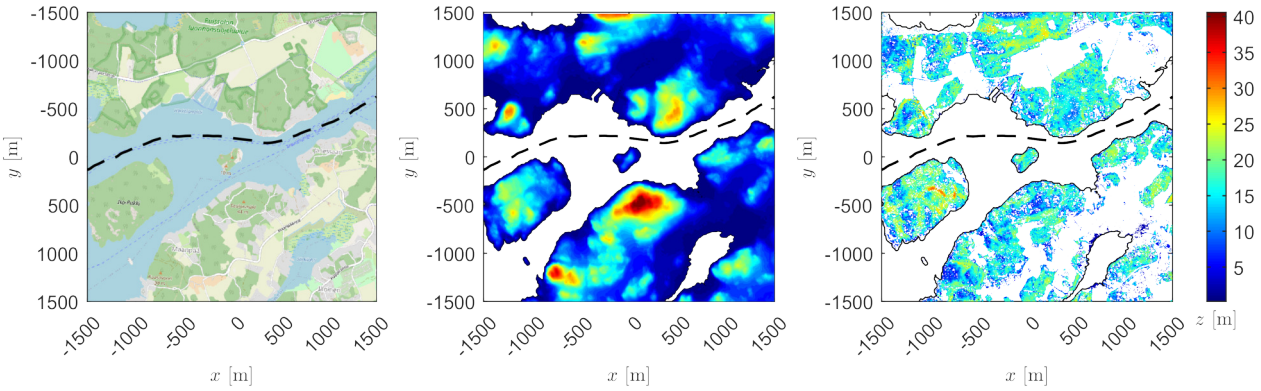

Figure 1: Map view of the site (left), terrain height (middle), and canopy height (right) for the region of interest (60°25′19.8"N, 22°09′48.8"E). The dashed line indicates the ship's route inside the fairway.

turbulence model (Shih et al., 1995), are solved in the present work to simulate the mean wind flow and Turbulent Kinetic Energy (TKE) over the site. Further, following the work of Shaw and Schumann (1992), the drag-force approach is used to model the effects of the forest in the numerical simulations. The total drag force F_i in the x_i direction in the momentum equations due to the forest is parameterized as

$$F_i = -C_d a_f |U| U_i, \; i = 1, 2, 3 \tag{1}$$

where a_f is the leaf biomass area per unit volume, also known as a Leaf Area Density (LAD), U_i is the wind speed in the x_i direction, $|U|$ is the magnitude of the velocity vector, and C_d is the leaf-level canopy drag coefficient taken here as 0.15 (Shaw & Schumann, 1992). Similarly, the source term for the TKE (k) equation is

$$F_k = \rho C_d a_f |U| \left[\beta_p |U|^2 - \beta_d k\right]. \tag{2}$$

Here, the constant $\beta_p = 0.17$ accounts for the production of turbulence due to the surface drag of canopy elements while $\beta_d = 3.37$ accounts for the enhanced dissipation. The source term for the TKE dissipation (ϵ) equation is given by

$$F_\epsilon = \rho C_d a_f |U| \epsilon \left[\frac{C_{\epsilon 4} \beta_p |U|^2}{k} - C_{\epsilon 5} \beta_d\right] \tag{3}$$

where $C_{\epsilon 4} = 0.9$ and $C_{\epsilon 5} = 0.9$ are the model constants. The approach used here to model the forests has been successfully used in several studies previously (Finnigan et al., 2009; Desmond & Watson, 2014; Agafonova et al., 2016a, 2016b; Adedipe et al., 2020, 2022) and it has been validated against measurements (Chaudhari et al., 2016a; Adedipe et al., 2020).

The LAD information (a_f) required in Equations (1)-(3) was extracted from the high-resolution laser-scanned point cloud data. This open-source data was obtained from the database of the National Land Survey of Finland (NSL, 2023). We used a recently developed method by Kamoske et al. (2019) that calculates LAD by counting the number of LiDAR pulses that enter and exit each voxel in a given vertical column, see Kamoske et al. (2019) for more details. The height of the detected vegetation canopy for the studied site is shown in Figure 1 (right), and the extracted canopy is in good agreement with the map view available in Figure 1(left).

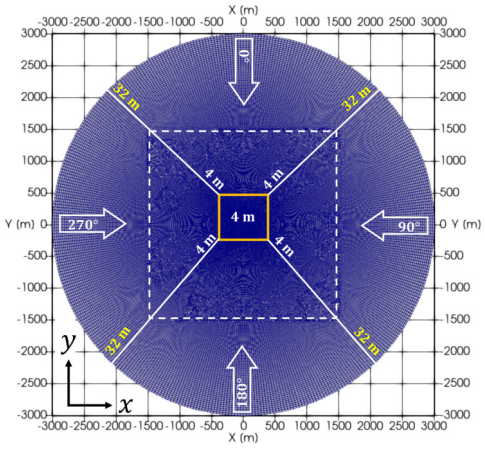

Figure 2: Top view of the CFD domain showing the meshing strategy, mesh resolutions, and approaching wind directions. The dashed square indicates the size of the topographic site.

The vegetation below 2 m was ignored here as their effects can not be resolved in the simulations due to the limitation of the CFD grid resolution. In brief, the height of the canopy on the site varies from 2 to 43.4 m while the mean height is 13.7 m above the ground level.

Computational Domain and Grid Spacing

We used a cylindrical-shaped computational domain to execute simulations for different wind directions without having to change the mesh, that is, within a single mesh. Figure 2 shows the top view of the computational domain with indications on the simulated site, mesh strategy, and incoming wind directions. The diameter of the computational domain was 6 km, and the height of the domain was 500 m, which is more than 10 times the maximum height of the terrain.

The dotted-square region in Figure 2 indicates the simulated topographic site, which is of the size of 3000×3000 m, as shown in Figure 1(middle). Following the concept of a virtual wind-tunnel (Janssen et al., 2017; Ricci et al., 2019, 2020), the simulated topographic site was placed in the center of the domain to allow a sufficient distance for the flow to adjust before approaching

Table 1: Mesh resolutions and other details from different grid cases. The CPU time is for simulations using 225 processors.

Case	2 m	4 m	8 m
Hori. resolution	2-32 m	4-32 m	8-32 m
Ver. resolution	2-24 m	2-24 m	2-24 m
Total grid cells	17 061 112	6 444 295	2 413 461
Mean error: U_x	-	0.3%	1.3%
Mean error: k	-	2.4%	11.8%
CPU time	2135 s	1211 s	469 s

the topography. The small solid-square region in the center of the domain, with the area of 400×400 m, indicates the region with the finest mesh resolutions in all three directions. Outside of this square region, the grid size gradually increases to 32 m toward the domain's outer (circular) boundary. In order to obtain grid-independent results, 3 different grid sizes, 2 m, 4 m, and 8 m, have been tested as the finest resolution in the horizontal directions (x and y). More details on the 3 grid cases are shown in Table 1.

The grid resolution in the vertical direction (z) was fixed in all 3 grid cases, however, it was non-uniform across that direction. Two separate grading factors were used to allow finer resolution in the lower part of the domain. Firstly, the vertical resolution varies from 2 m near the water/terrain surface to 4 m at the height of 100 m. Above this height, it varies from 4 to 24 m at the top of the domain. In the literature, similar grid resolutions have been used for simulating the atmospheric flows over complex terrains (Kim & Patel, 2000; Castro et al., 2003; Bechmann & Sørensen, 2010), forests (Shaw & Schumann, 1992; Dalpé & Masson, 2008; Nebenführ & Davidson, 2015) and real urban areas (Xie, 2011; Auvinen et al., 2020).

Boundary Conditions and Numerical Settings

All the numerical simulations were carried out by imposing the fully-developed profiles (not shown in this article) for U, k, and ϵ at the inflow plane. Following Castro et al. (2003), these profiles have been obtained from a separate precursor simulation of wind flows over a flat terrain having a wind speed of 8.23 m/s at the height of 10 m. The circular horizontal boundary was split from the center of the domain into two boundaries: inflow and outflow. In this way, the first half represents the inflow plane and the other half the outflow boundary. At the outflow plane, the pressure field was fixed to zero value while a Neumann boundary condition, with zero gradients, was used for the rest of the flow variables. The slip boundary condition was used for all the flow variables on the top boundary. The lower boundary is also split into two, water and terrain boundaries. Following Berg et al. (2011), the roughness length (z_0) for the water and terrain surfaces was used as 0.0003 m and 0.015 m, respectively. On the lower boundary, the wall functions typically used for the atmospheric flows (Kim & Patel, 2000; Castro et al., 2003; Vuorinen et al., 2015; Chaudhari et al., 2018) are applied for U, k, and ϵ fields.

The numerical simulations were carried out using a well-known open-source platform, OpenFOAM, with version v2012 (OpenCFD, 2020). The mesh generation was performed using *SnappyHexMesh* which is also OpenFOAM's mesh generation tool. The governing equations were discretized in space using two schemes. The advection term was discretized using the second-order upwind scheme, while the gradient and laplacian terms were using the second-order central differencing scheme.

Grid Sensitivity Analysis

The grid sensitivity was evaluated by comparing CFD predictions obtained with different grid resolutions. Figure 3 shows the x-directional velocity (U_x) and TKE (k) at 10 m height above the water level on the route (as indicated in Figure 1) for the 270° Wind Direction (WD). Firstly, it can be observed that the results from the 2 m and 4 m cases are qualitatively close to each other for most of the route. The results from the 8 m case deviate slightly, for example, from $x = -1000$ to 750 m, when compared to the other two cases. To have a quantitative analysis, we calculated the mean (over all the points on the route) relative error with respect to the 2 m case which is having the highest number of grid cells. The errors for U_x and k are presented in Table 1. The error for the 4 m case was only 0.3% for U_x and 2.4% for k. Consequently, the 4 m was selected as the finest horizontal resolution when performing simulation for all WDs.

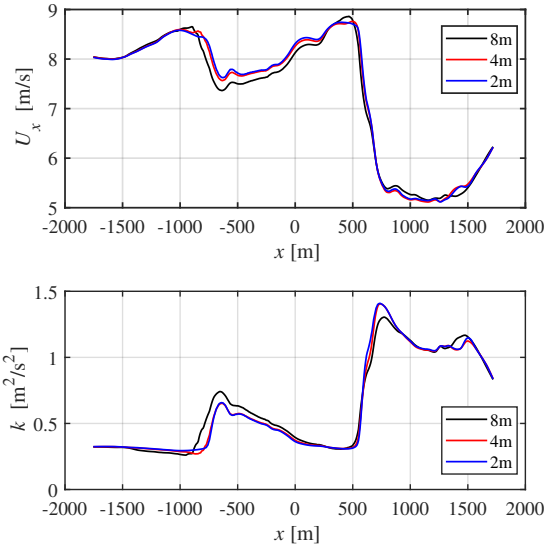

Figure 3: Velocity (upper) and TKE (lower) predictions at 10 m above the water level for CFD simulations with different grid resolutions. The results are presented for the 270° WD.

VALIDATION OF THE CFD MODEL

Since wind measurements are not available for the given site, we had to use another site to validate the CFD model and the used numerical approach. We chose a well-known measurement site, the Askervien hill (Taylor & Teunissen, 1987), located in Scotland. The Askervien

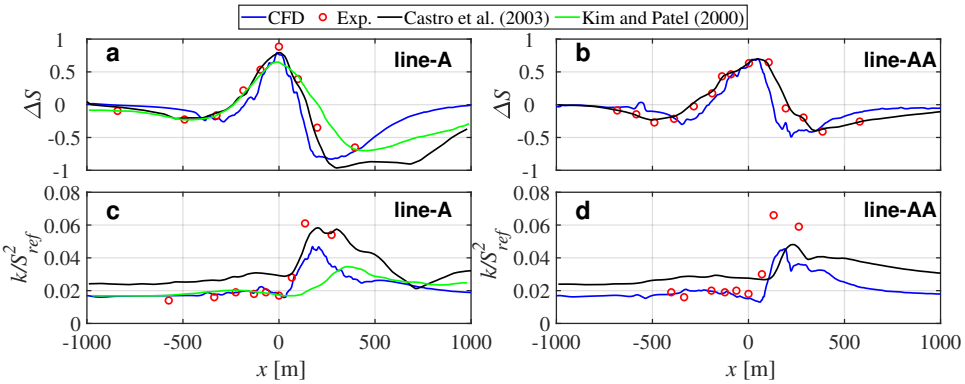

Figure 4: CFD prediction of speed-up and TKE at 10 m above the ground level compared against measurements and other numerical predictions from the literature.

hill is 116 m high from the local ground with minor and major axes of roughly 1000 and 2000 m. It has a nearly elliptical shape with a maximum slope of 30°. During the measurements campaign, more than 50 towers were deployed in three linear arrays, one parallel and two perpendiculars (lines B, A, and AA to the hill's major axis, see. Taylor and Teunissen (1987). The amount of measured data provides a detailed description of the near-surface wind, making the site well suited for validating numerical models (Castro et al., 2003; Kim & Patel, 2000; Bechmann & Sørensen, 2010).

Our validation setup used a similar approach for the computational domain, the grid sizes, the boundary conditions, and the numerical schemes. However, as the size of the Askervien hill is much larger, the diameter of the domain was increased to 8 km and the height of the domain to 700 m, as also used by Castro et al. (2003). Similarly, the horizontal mesh resolution varied from 4 to 40 m, and the vertical one from 2 to 32 m, resulting in 9 454 915 grid cells in total.

Figure 4 compares our numerical results with the measurements (Taylor & Teunissen, 1987) and other numerical predictions from the literature (Castro et al., 2003; Kim & Patel, 2000). The figure shows the non-dimensional speed-up ΔS and normalized TKE $\left(k/S_{ref}^2\right)$ at 10 m above the ground level for lines A and AA, with ΔS defined as:

$$\Delta S(z) = \frac{S(z) - S_{ref}(z)}{S_{ref}(z)}, \tag{4}$$

where S is the magnitude of the horizontal velocities (U_x and U_y), and S_{ref} is the magnitude velocity from the reference (i.e., inflow) location. Overall, our numerical results satisfactorily reproduce the mean wind speed and turbulence quantities near the surface of the Askervien hill, and furthermore, the results are in qualitative agreement with the measurements and other numerical predictions at most of the locations. Therefore, we believe that our CFD approach can produce satisfactory results for the site in the Turku archipelago, which has less complex features than the Askervien hill.

RESULTS AND DISCUSSION

We have used CFD simulations to predict the local wind flows over a portion of the fairway in the Turku archipelago. The simulated site is just outside the port of Turku. All simulations were carried out in the presence and absence of forests in order to study the influence of the surrounding forests for the given site. For both scenarios (that is, with and without the forests), the simulations were performed for 4 different WDs, 0° (North), 90° (East), 180° (South), and 270° (West).

Wind and Turbulence Distributions Along the Fairway

Our main goal for this study was to predict the local wind flows over and along the fairway in the archipelago and to evaluate the effects of terrain and forests in particular. The results in Figures 5 and 6, which show the horizontal wind speed (S) and TKE (k) at 10 m height above the water level, highlight the qualitative distributions of the flow quantities for all 4 WDs. The results utilizing the terrain-only (upper rows) conditions exhibit mainly small deviations from the inflows, with changes primarily located in the wake regions for each WD, where the wind speed is reduced and the TKE is increased. The introduction of forests similarly leads to decreased wind speeds and increased turbulence on average, but the effects are clearly larger and can be observed over the majority of the water area. Consequently, incorporating forests leads to clearly larger variations in wind speeds over the water, while at the same time introducing steep transitions in wind speeds over fairly short distances that can be treacherous for safe passage. This can be observed for winds in all directions. For the easterly and westerly winds (90° and 270°), the steep transition in wind speeds occurs on the border region of the fairway. However, for the northerly and southerly winds (0° and 180°), the transition occurs along the fairway where it will cause the lateral wind force on vessels to vary strongly with the location along the fairway.

Speed-up and Turbulence Intensity

We analyzed the results along the fairway (black dashed lines in Figure 1) in more detail to get a more quantitative analysis of the winds affecting a vessel

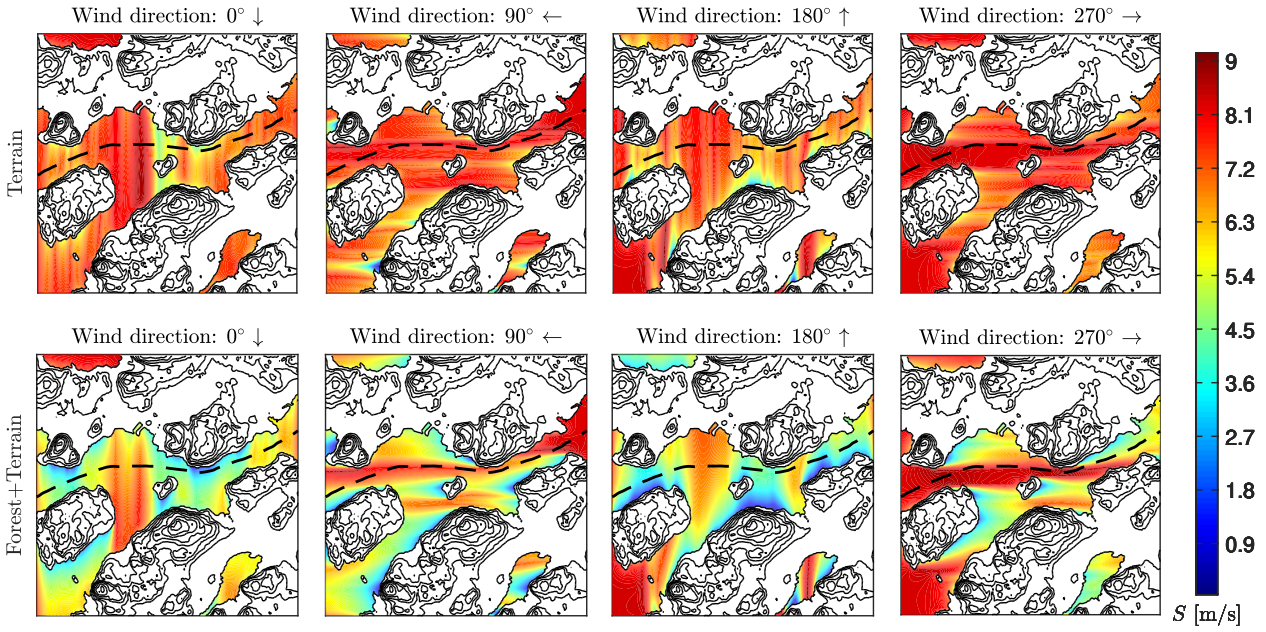

Figure 5: Contours of the wind speed S at 10 m above the water level for various wind directions in the region of interest (cf. Figure 1). The terrain contour interval is 5 m. The dashed line indicates the route of vessels.

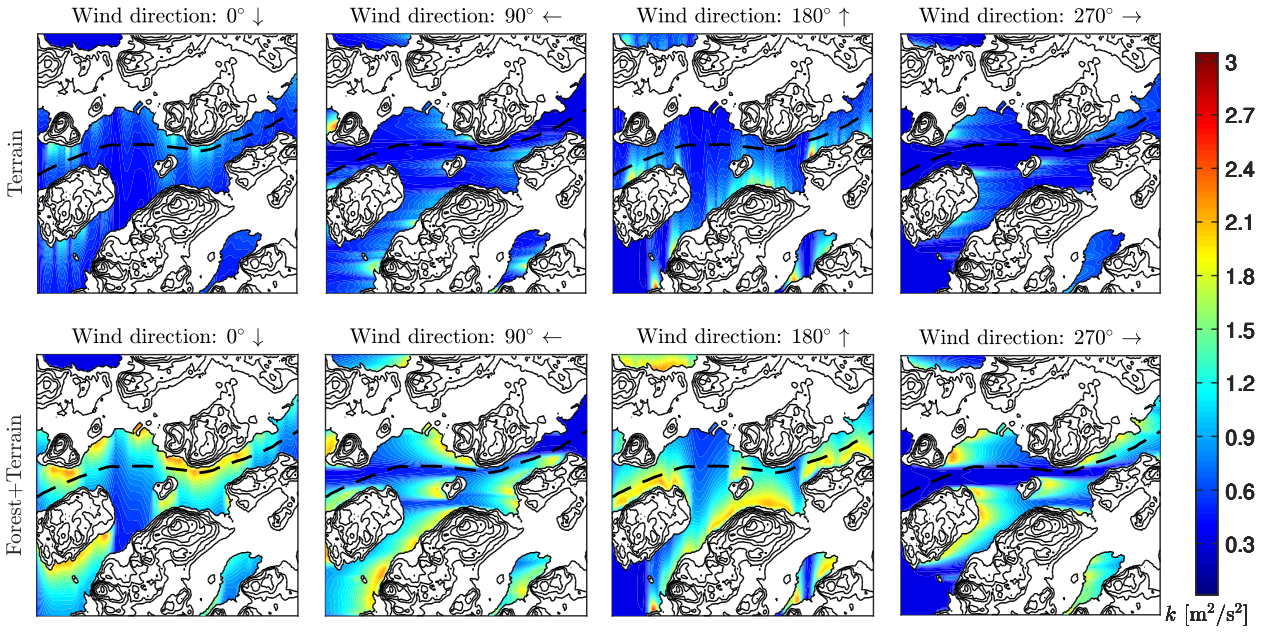

Figure 6: Contours of the TKE k at 10 m above the water level for various wind directions in the region of interest (cf. Figure 1). The terrain contour interval is 5 m. The dashed line indicates the route of vessels.

that passes through the archipelago. Figure 7 shows the speed-up (Equation (4)) and the normalized Turbulence Intensity (TI), I/I_{ref}, at 10 m above the water level along the fairway for both conditions (with and without the forests) and for all 4 WDs. The reference, I_{ref}, for the normalized TI, is given by the inflow. The speed-up and the normalized intensity thus compare the observed effects with respect to the inflow for both conditions. As expected from Figures 5 and 6, the surrounding forests caused a reduction in the wind speed (negative ΔS) but an increment in the TI ($I/I_{ref} > 1$). The forest effects along the fairway are strongest for northerly and southerly (0° and 180°) winds, for which the speed-up decreased to -0.8 with forests included (at $x = 300$ m; Figure 7(a)). The lowest speed-up in the absence of forests (i.e. only terrain) was in turn -0.44 (at $x = -97$ m; Figure 7(a)). The normalized TI appears negatively correlated wind the speed-up, and the maximal values are found along the locations of the fairway with the lowest speed-up (i.e. $x = 300$ m for northerly winds, 0°). At its peak, the normalized TI reached up to 14 times the reference level with forests,

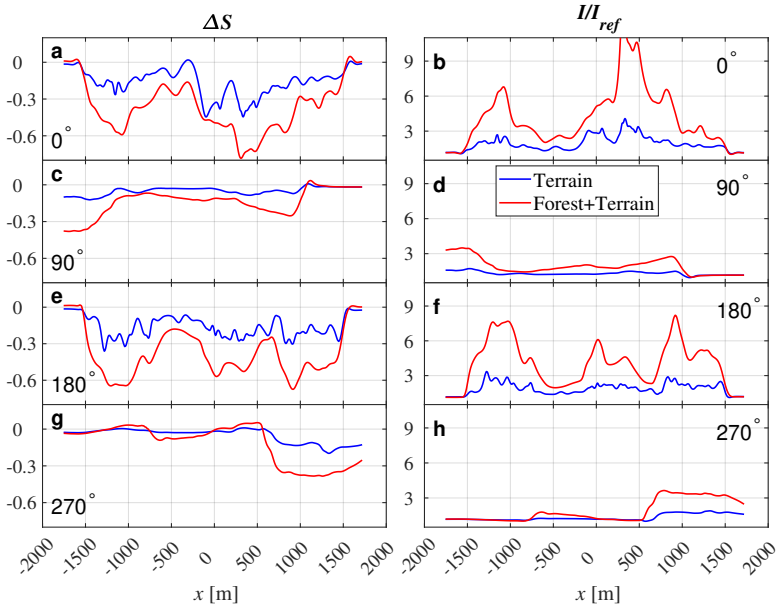

Figure 7: Non-dimensional speed-up and TI at 10 m above the water level on the route for the 4 WDs.

but only 3.5 times the reference level in the absence of forests (Figure 7(b)).

We further computed the mean and standard deviation values for both, the speed-up and the TI, to get a quantitative measure of the effects along the whole fairway in the studied region. These statistics are presented in Figure 8. The results show that the mean speed-up from the terrain-only condition is similar between the 0° and 180° (~ -0.16) WDs, and between the 90° and 270° (~ -0.05) WDs. This indicates that the terrain slows down the wind speed along the fairway by 16% on average (Figure 8(a)) for 0° and 180° winds and by 5% for the other two winds. At the same time, the terrain increased the TI for all WDs by 60–100%.

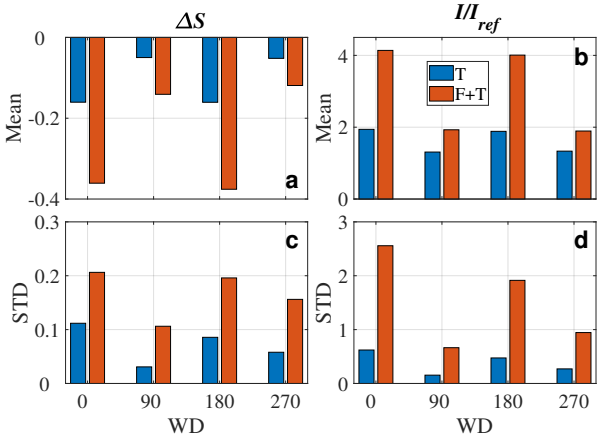

Figure 8: Mean and standard deviation (STD) of the speed-up and TI for the 4 WDs. In the legend, T stands for Terrain and F for Forest.

The average speed-up with forests included is generally lower for all WDs. For example, terrain and forests together slow down the wind speeds by roughly 38% for 0° and 180° WDs, and by 14% and 12% for 90° and 270° WDs, respectively (Figure 8(a)). This is due to the fact that forests extract momentum from the wind and, as a result, the wind profile has more shear (Nebenführ & Davidson, 2015; Adedipe et al., 2022). Consequently, the wind speed will decrease, especially at lower heights. High wind-shear generally also leads to an increment in turbulence and, for the same reason, the mean increment in the TI is reaching up to 4 times the inflow intensity for 0° and 180° WDs. The mean turbulence increase for the other two WDs is about 90% (Figure 8(b)).

The STD values, presented in Figure 8(c) and (d), are quite informative for understanding the variability in the local flow. It has been observed that the ratio between the STD and mean values is generally higher, especially for the speed-up. This indicates high variability in the wind speed due to the surrounding terrain/forest conditions, which is typical in archipelagos. For the speed-up, the ratio is similar between the terrain and combined (terrains and forests) conditions, whereas, for the TI, the ratio is higher (by 2-3 times) for the combined surface conditions (Figure 8(d)). This indicates stronger variations and sensitivity in the local turbulence due to the forests. As a result, the wind loads on a ship will be more frequent as the ship travels further in such a complex environment that is typical in archipelagos.

Forest Effects at Various Heights

Next, we normalized the results from the combined (forest and terrain) condition with the results from the terrain-only condition ($S_{\mathrm{F+T}}/S_{\mathrm{T}}$ and $I_{\mathrm{F+T}}/I_{\mathrm{T}}$). The resulting mean and STD values along the fairway are shown in Figure 9 for three different heights (10, 20, and 30 m). The mean velocity ratio ($S_{\mathrm{F+T}}/S_{\mathrm{T}}$) is ranging from 0.7 to 0.9 depending on the WD, but the ratios do not vary for any of the studied heights (Figure 9(a)). This indicates that, on average, the forests have a similar impact level on all three heights. The STD values of the ratios, nonetheless, show a slight decrement with height,

indicating lesser fluctuations in the forest effects along the route for increasing heights (Figure 9(c)).

The mean values for the normalized TI increase with the height (Figure 9(b)), indicating that the forest effects on turbulence get stronger higher up. On average, the surrounding forests increase the TI by 2-3 times for 0° and 180° WDs, and by 1.3 to 1.8 times for 90° and 270° WDs (Figure 9(b)). The STD values also increase with height, revealing the increasing variability in the TI with height due to various forest patches along the fairway.

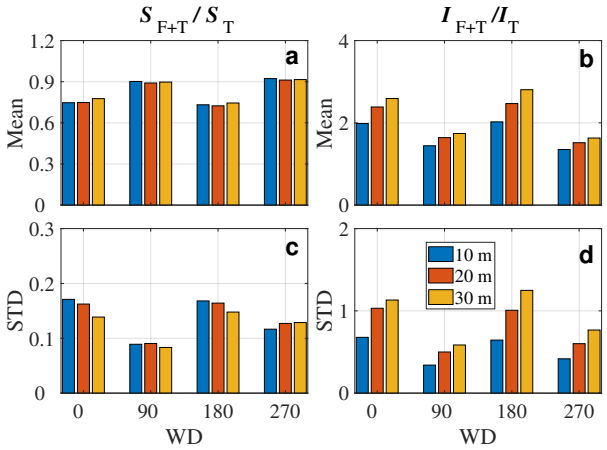

Figure 9: Mean and standard deviation (STD) of the normalized wind speed and TI for the 4 WDs.

Since the forest effects generally get stronger at each of the three heights studied in Figure 9(b) and (d), it was deemed necessary to investigate how high up the forest effects are present along the route. For this, we selected three individual locations and present the normalized results as a function of heights in Figure 10. Among the three locations, two locations $(x = -1100, y = 66)$ m and $(306, 159)$ m are having significant forest effects according to Figures 7 and the third location is the center of the route. It can be noticed that the forests affect the local wind and turbulence profiles as high as 170 to 200 m depending on the WD and the location. The forest impact is, however, most prominent within the height range 0-30 m, which corresponds to the relevant range for a typical large vessel passing through the archipelago. Also, the 270° wind stands out in Figure 10 by being affected less by forests, but this is simply due to the east-west going fairway being open from that direction.

Forest Density and Turbulence

The impact of forests depends on the size, the height of the trees, and the forest density (LAI) (Adedipe et al., 2022). Previously, it has been seen that a dense homogeneous forest can increase the turbulence level by 4-5 times above the forest edge compared to a no-forest case (Nebenführ & Davidson, 2014; Adedipe et al., 2020). This is in agreement with our results. Furthermore, Adedipe et al. (2020) studied the relation between the forest density and turbulence level in a systematic way. They concluded that extremely sparse (LAI $<$ 0.5) and dense (LAI $>$ 5) forests result in

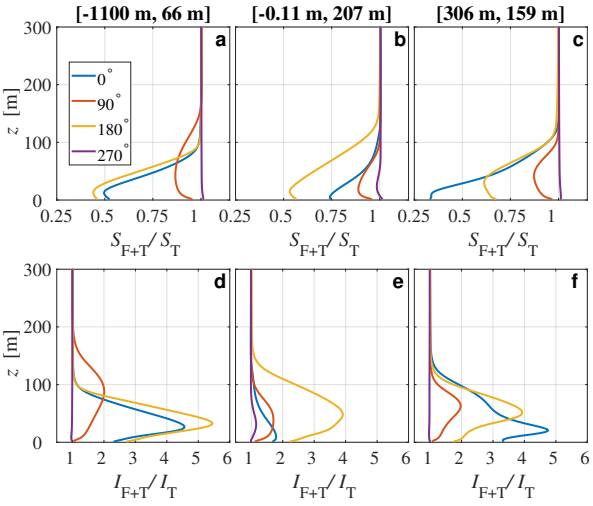

Figure 10: Vertical profiles of the normalized horizontal wind speed (top) and TI (bottom) at 3 selected locations on the route.

similar turbulence levels at the hub height of wind turbines ($\sim$ 100 m), and that a forest having intermediate density (0.5 $<$ LAI $<$ 5) results in the maximum turbulence level. For the region studied here, the LAI ranges from 0.01 to 3 while the mean value is 0.6. The large forest effects observed here are thus in line with previous works. It is also useful to notice that the tree height is as high as the highest terrain in the studied region (Figure 1) and that the canopy layer will percentwise be located much higher up than the terrain in many areas.

CONCLUSIONS

In this work, we incorporated a digital elevation model and forest canopy model together into a well-known open-source platform, OpenFOAM, and carried out CFD simulations to analyze the wind flows over a region of interest in the Turku Archipelago. Wind flows over the site were simulated with and without surrounding forests to evaluate the impact of forests on local wind speeds and turbulence. Our results show that forests could, in some areas of the studied site, reduce the wind speed to one-third whereas the turbulence level increases six times compared to the terrain-only conditions. The impact of the forests varies with wind direction and surrounding terrain/forest properties, with the most significant impact observed with winds from the north or south. Further, it has been revealed that the impact of the forest reaches up to 200 m above the water level. This implies that all sizes of vessels are affected by the increased fluctuations in the wind. While the reduced wind speed would lead to smaller forces acting on a ship, the large variation seen along the fairway may lead to sudden changes in local wind flows that can be surprising or even dangerous. Moreover, the increased turbulence level may lead to increased vibrations with more energetic forces than anticipated.

The study concludes that forests play a vital role in local wind flows and should be considered when assessing wind conditions for the safe passage of ships

through archipelagos. Through the simulation results presented in this paper, we have shown that CFD modeling can be used as a tool for aiding future smart fairway systems in estimating the local wind condition, thus improving overall situational awareness. In future work, the presented simulation method can be applied to other areas of interest in the archipelago, such as ports and passages where precise maneuvers are required. By doing so, a complete picture of the wind patterns in fairways can be formed, allowing operational limits of vessels to be assessed for varying wind conditions and helping to ensure the safe passage of ships through the archipelago.

ACKNOWLEDGMENTS

This research was carried out using the financial support from the Applied Research Platform for Autonomous Systems (ARPA) project at Turku University of Applied Sciences (TUAS) and Novia University of Applied Sciences. Additional financial support was also received from the Intelligent and Sustainable Stormwater Management (ISMO) project at TUAS. Both projects were funded by the Finnish Ministry of Education and Culture. During this work, the high-performance computing resources were provided by CSC-IT Center for Science Ltd, in Espoo, Finland.

REFERENCES

Adedipe, T., Chaudhari, A., Hellsten, A., Kauranne, T., & Haario, H. (2022). Numerical investigation on the effects of forest heterogeneity on wind-turbine wake. *Energies*, *15*(5), 1896.

Adedipe, T., Chaudhari, A., & Kauranne, T. (2020). Impact of different forest densities on atmospheric boundary-layer development and wind-turbine wake. *Wind Energy*, *23*(5), 1165-1180.

Agafonova, O., Avramenko, A., Chaudhari, A., & Hellsten, A. (2016a). The effects of the canopy created velocity inflection in the wake development. *AIP Conference Proceedings*, *1738*(1), 480082.

Agafonova, O., Avramenko, A., Chaudhari, A., & Hellsten, A. (2016b). Effects of the canopy created velocity inflection in the wake development in a large wind turbine array. *Journal of Physics: Conference Series*, *753*(3), 032001.

Auvinen, M., Boi, S., Hellsten, A., Tanhuanpaa, T., & Jarvi, L. (2020). Study of realistic urban boundary layer turbulence with high-resolution large-eddy simulation. *Atmosphere*, *11*(2).

Bechmann, A., & Sørensen, N. N. (2010). Hybrid RANS/LES method for wind flow over complex terrain. *Wind Energy: An International Journal for Progress and Applications in Wind Power Conversion Technology*, *13*(1), 36–50.

Berg, J., Mann, J., Bechmann, A., Courtney, M., & Jørgensen, H. E. (2011). The Bolund experiment, Part i: Flow over a steep, three-dimensional hill. *Boundary-Layer Meteorology*, *141*, 219–243.

Blocken, B., van der Hout, A., Dekker, J., & Weiler, O. (2015). CFD simulation of wind flow over natural complex terrain: Case study with validation by field measurements for Ria de Ferrol, Galicia, Spain. *Journal of Wind Engineering and Industrial Aerodynamics*, *147*, 43–57.

Castro, F. A., Palma, J., & Silva Lopes, A. (2003). Simulation of the askervein flow. Part 1: Reynolds Averaged Navier–Stokes Equations ($\kappa - \epsilon$ turbulence model). *Boundary-Layer Meteorology*, *107*, 501–530.

Chaudhari, A., Conan, B., Aubrun, S., & Hellsten, A. (2016a). Numerical study of how stable stratification affects turbulence instabilities above a forest cover: application to wind energy. *Journal of Physics: Conference Series*, *753*(3), 032037.

Chaudhari, A., Hellsten, A., & Hämäläinen, J. (2016). Full-scale experimental validation of large-eddy simulation of wind flows over complex terrain: The Bolund hill. *Advances in Meteorology*, *2016*. (Article ID: 9232759)

Chaudhari, A., Vuorinen, V., Agafonova, O., Hellsten, A., & Hämäläinen, J. (2014). Large-eddy simulation for atmospheric boundary layer flows over complex terrains with applications in wind energy. In A. Huerta, E. Onate, & X. Oliver (Eds.), *11^{th} World Congress on Computational Mechanics, WCCM2014* (p. 5205-5216). Barcelona, Spain.

Chaudhari, A., Vuorinen, V., Hämäläinen, J., & Hellsten, A. (2018). Large-eddy simulations for hill terrains: validation with wind-tunnel and field measurements. *Computational & Applied Mathematics*, *37 (2)*, 2017 - 2038.

Conan, B., Chaudhari, A., Aubrun, S., Beeck, J., Hämäläinen, J., & Hellsten, A. (2016). Experimental and numerical modelling of flow over complex terrain: The Bolund hill. *Boundary-Layer Meteorology*, *158*(2), 183–208.

Dalpé, B., & Masson, C. (2008). Numerical study of fully developed turbulent flow within and above a dense forest. *Wind Energy*, *11*(5), 503-515.

Desmond, C. J., & Watson, S. (2014). A study of stability effects in forested terrain. *Journal of Physics: Conference Series*, *555*, 012027.

Dhunny, A., Lollchund, M., & Rughooputh, S. (2017). Wind energy evaluation for a highly complex terrain using Computational Fluid Dynamics (CFD). *Renewable Energy*, *101*, 1–9.

Finnigan, J. J., Shaw, R. H., & Patton, E. G. (2009). Turbulence structure above a vegetation canopy. *Journal of Fluid Mechanics*, *637*, 387–424.

Immonen, E., Bengs, D., Manngård, M., & Westö, J. (2022). Automated geometry and hexahedral mesh generation for kilometer-scale atmospheric flow simulations. *Rakenteiden Mekaniikka*, *55*(4), 81–94.

Janssen, W., Blocken, B., & van Wijhe, H. (2017). CFD simulations of wind loads on a container ship: Validation and impact of geometrical simplifications. *Journal of Wind Engineering and Industrial Aerodynamics*, *166*, 106–116.

Jones, D., Snider, C., Nassehi, A., Yon, J., & Hicks, B. (2020). Characterising the digital twin: A systematic literature review. *CIRP Journal of Manufacturing Science and Technology*, *29*, 36–52.

Kamoske, A. G., Dahlin, K. M., Stark, S. C., & Serbin, S. P. (2019). Leaf area density from airborne lidar: Comparing sensors and resolutions in a temperate broadleaf forest ecosystem. *Forest Ecology and Management*, *433*, 364-375.

Kanarik, H., Tuomi, L., Alenius, P., Lensu, M., Miettunen, E., & Hietala, R. (2018). Evaluating strong currents at a fairway in the Finnish Archipelago Sea. *Journal of Marine Science and Engineering*, *6*(4), 122.

Kim, H.-G., & Patel, V. (2000). Test of turbulence models for wind flow over terrain with separation and recirculation. *Boundary-Layer Meteorology*, *94*, 5–21.

Koop, A., Rossin, B., & Vaz, G. (2012). Predicting wind loads on typical offshore vessels using CFD. In *International Conference on Offshore Mechanics and Arctic Engineering* (Vol. 44922, pp. 731–742).

Kritzinger, W., Karner, M., Traar, G., Henjes, J., & Sihn, W. (2018). Digital twin in manufacturing: A categorical literature review and classification. *IFAC-PapersOnline*, *51*(11), 1016–1022.

Nebenführ, B., & Davidson, L. (2014). Influence of a forest canopy on the neutral atmospheric boudary layer-a LES study. In *ETMM10: 10^{th} International ERCOFTAC Symposium on Turbulence Modelling and Measurements.*

Nebenführ, B., & Davidson, L. (2015). Large-eddy simulation study of thermally stratified canopy flow. *Boundary-Layer Meteorology*, *156*(2), 253–276.

NSL. (2023). *National land survey of Finland.* Retrieved 2023-02-24, from `https://tiedostopalvelu.maanmittauslaitos.fi/tp/kartta?lang=en`

OpenCFD. (2020). *OpenCFD Release OpenFOAM.* Retrieved 2023-01-30, from `https://www.openfoam.com/news/main-news/openfoam-v20-12`

Ravensbergen, M., Helgedagsrud, T., Bazilevs, Y., & Korobenko, A. (2020). A variational multiscale framework for atmospheric turbulent flows over complex environmental terrains. *Computer Methods in Applied Mechanics and Engineering*, *368*, 113182.

Ricci, A., Burlando, M., Repetto, M., & Blocken, B. (2019). Simulation of urban boundary and canopy layer flows in port areas induced by different marine boundary layer inflow conditions. *Science of The Total Environment*, *670*, 876-892.

Ricci, A., Janssen, W., van Wijhe, H., & Blocken, B. (2020). Cfd simulation of wind forces on ships in ports: Case study for the Rotterdam cruise terminal. *Journal of Wind Engineering and Industrial Aerodynamics*, *205*, 104315.

Ricci, A., Vasaturo, R., & Blocken, B. (2023). An integrated tool to improve the safety of seaports and waterways under strong wind conditions. *Journal of Wind Engineering and Industrial Aerodynamics*, *234*, 105327.

Shaw, R. H., & Schumann, U. (1992, Oct 01). Large-eddy simulation of turbulent flow above and within a forest. *Boundary-Layer Meteorology*, *61*(1), 47–64.

Shih, T.-H., Liou, W. W., Shabbir, A., Yang, Z., & Zhu, J. (1995). A new $\kappa - \epsilon$ eddy viscosity model for high Reynolds number turbulent flows. *Computers & Fluids*, *24*(3), 227-238.

Taylor, P., & Teunissen, H. (1987). The Askervein Hill project: overview and background data. *Boundary-Layer Meteorology*, *39*, 15–39.

Temel, O., Bricteux, L., & van Beeck, J. (2018). Coupled WRF-OpenFOAM study of wind flow over complex terrain. *Journal of Wind Engineering and Industrial Aerodynamics*, *174*, 152-169.

Vuorinen, V., Chaudhari, A., & Keskinen, J.-P. (2015). Large-eddy simulation in a complex hill terrain enabled by a compact fractional step OpenFOAM solver. *Advances in Engineering Software*, *79*(0), 70 - 80.

Xie, Z.-T. (2011). Modelling street-scale flow and dispersion in realistic winds—towards coupling with mesoscale meteorological models. *Boundary-Layer Meteorology*, *141*, 53–75.

AUTHOR BIOGRAPHIES

Ashvin Chaudhari D.Sc. (Tech.) is a Researcher at Computational Engineering and Analysis (COMEA) research group, Turku University of Applied Sciences, Finland. He studied Fluid Dynamics and Applied Mathematics and received his doctoral degree in Technology from LUT University (Finland) in 2014. For over a decade, he has been working on modeling and simulations of atmospheric flows over various surface conditions, such as complex terrains and urban areas, for various applications. Email: `Ashvin.Chaudhari@turkuamk.fi`

Eero Immonen D.Sc. (Tech.) and Adjunct Professor, is a leader of the Computational Engineering and Analysis (COMEA) research group at Turku University of Applied Sciences, Finland. E-mail: `Eero.Immonen@turkuamk.fi`

Mikael Manngård M.Sc. (Tech.) is a Project Manager at Novia University of Applied Sciences, Finland. He is pursuing his Ph.D. degree in Process Control at Åbo Akademi University, Finland. E-mail: `mikael.manngard@novia.fi`

Johan Westö D.Sc. (Tech.) is a Project Manager at Novia University of Applied Sciences, Finland. E-mail: `johan.westo@novia.fi`

Dennis Bengs B.Sc. (Tech.) is a laboratory engineer at Novia University of Applied Sciences, Finland. E-mail: `dennis.bengs@novia.fi`